

Naïve PAINE: Lightweight Text-to-Image Generation Improvement with Prompt Evaluation

Joong Ho Kim¹, Nicholas Thai¹, Souhardya Saha Dip¹,
Dong Lao², and Keith G. Mills¹
{jkim5, nthai4, ssahad1, dong.lao, keith.mills}@lsu.edu

¹ LSU ATHENA Lab, Baton Rouge, LA, U.S.A. 70803

² LSU Vision Lab, Baton Rouge, LA, U.S.A. 70803

Abstract. Text-to-Image (T2I) generation is primarily driven by Diffusion Models (DM) which rely on random Gaussian noise. Thus, like playing the slots at a casino, a DM will produce different results given the same user-defined inputs. This imposes a gambler’s burden: To perform multiple generation cycles to obtain a satisfactory result. However, even though DMs use stochastic sampling to seed generation, the distribution of generated content quality highly depends on the prompt and the generative ability of a DM with respect to it.

To account for this, we propose Naïve PAINE for improving the generative quality of Diffusion Models by leveraging T2I preference benchmarks. We directly predict the numerical quality of an image from the initial noise and given prompt. Naïve PAINE then selects a handful of quality noises and forwards them to the DM for generation. Further, Naïve PAINE provides feedback on the DM generative quality given the prompt and is lightweight enough to seamlessly fit into existing DM pipelines. Experimental results demonstrate that Naïve PAINE outperforms existing approaches on several prompt corpus benchmarks. Code available at <https://github.com/LSU-ATHENA/Naive-PAINE>.

Keywords: Diffusion Models · Text-to-Image Synthesis · Prediction

1 Introduction

Using computers to realize artwork from human thoughts has been a long-standing goal of Artificial Intelligence (AI) [14, 56, 58]. Once delegated to science fiction, this task is being realized by AI generated content (AIGC) models [23, 67, 76], among which latent Diffusion Models (DM) [4, 6, 10, 12, 18, 44, 63, 68, 85] are arguably the most notorious class in terms of open-source impact [13, 36, 60].

However, interacting with a diffusion model can feel surprisingly similar to playing the slots in a casino. The user makes some initial choices, such as providing a textual prompt or picking which machine to sit in front of. Then, once the lever is pulled, the sampler begins its stochastic process [28, 73, 74], and one counts the timesteps. If the result is unsatisfactory, the instinctual choice is to

pull the lever again [17, 21], yet each attempt consumes resources: casino tokens in Las Vegas, computational energy on a GPU, and in both cases, time. The governing principle is the same: every outcome begins from randomness, and every additional trial carries a cost.

This cost is incurred because DMs, like slot machines, have inherent stochasticity that imposes a non-negligible impact on generative performance [34, 59, 78, 81] in terms of qualitative image perception [87] and quantitative metrics [22]. However, just as gamblers, arguably some of the most persistent data engineers, have historically attempted to reverse engineer random number generators to make slot machines predictable [39, 71], there are recent developments which can improve the output quality of DMs via initial noise optimization. Such approaches may mutate the initial noise [77, 80, 90] or adopt prompt manipulation [30, 31, 33] and image editing [89] ideas to alter generation [2, 8, 9, 24].

However, a key limitation of current literature is that DM generative performance strongly depends on the prompt, as we show in Section 2.3. Specifically, while there are several prompt-based T2I benchmarks [22, 38, 50, 84] which aim to quantify a human’s preference for a given image with respect to the prompt, these are finite compared to the scope of human imagination. Moreover, modeling human preference is an inherently noisy task [29, 51, 86], benchmark performance is not all you need. Rather, before a gambler reverse engineers a casino slot machine, they should first determine *which* slot machine yields the best jackpot.

We cast this issue as a research question: *Given an initial noise, can one estimate how good the output is likely to be without executing the entire denoising process?* We answer this question with Naïve PAINE, or Naïve Prompt-Aware Initial Noise Evaluator, a lightweight, plug-and-play method that achieves initial noise optimization whilst also providing valuable and interpretable feedback on how well a DM can generate desired content. Specifically, Naïve PAINE short-circuits DM generation to estimate the performance of a would-be AI image from the initial stochastic noise that would seed generation. Further, we design our method to provide interpretable feedback on how hard a given prompt would be to generate. Our detailed contributions are as follows:

First, we cast the problem of initial noise optimization as a scalar prediction regression task. We construct PAINE as a predictor model that estimates the performance of DM-generated images from the prompts and initial noise tensors that are inputs to the process. Unlike more intensive [19, 20, 43] or guided [8, 24, 77] approaches, PAINE is DM-agnostic, adapts to the usage of multiple prompt text encoders, and does not alter DM generation or require fine-tuning.

Second, we conduct a study on the influence that the prompt, noise and DM itself have on benchmark metric distributions in Section 2.3. We find that the prompt significantly determines the distribution of scores, i.e., some prompts are more difficult to generate than others. Further, although sampling a noise serves to sample from the preference metric distribution, the most/least optimal noise varies with each prompt. Different from existing literature [77, 80, 90] which may mutate the noise to maximize performance for the prompt, we take inspiration from Bayes’ Theorem [3, 64] and design our method to also provide a *prior*

measure of how well a DM can generate an image for a given prompt regardless of what noise is given, giving rise to Naïve PAINE.

Third, Naïve PAINE is both computationally lightweight and imposes a smaller inference latency overhead than existing methods [90] on various hardware. Further, it is easy to deploy in various DM pipelines and workflows, whether as directly part of a codebase such as Diffusers [62] or easily integrated into a more complex GUI-based framework like ComfyUI [15, 88] and others [1].

Through extensive experiments we demonstrate that Naïve PAINE achieves superior initial noise optimization in terms of quantitative benchmarks and qualitative generation results, whilst also providing accurate and interpretable prompt-performance feedback. To prove the generalizability of our method we test on several popular T2I DMs including SDXL [63], DreamShaper [47], Hunyuan [44] and PixArt- Σ [10], outperforming other contemporary lightweight approaches [90] in terms of prompt-adherence and preference metrics [50, 84].

2 Background & Related Work

Diffusion Models (DM) generate content by initially sampling a Gaussian noise $X_T \in \mathbb{R}^{H \times W \times C} \sim \mathcal{N}(0, 1)$ which is gradually refined using the reverse diffusion process (RDP) [73]. Most Text-to-Image (T2I) DMs [10, 18, 44, 63, 85] operate in a latent embedding space [68] of a VAE [37] encoder/decoder pair where H , W and C correspond to VAE height, width and channel embedding dimensions, respectively. The RDP is iterative, where at every timestep t , a scheduler computes X_{t-1} from X_t , i.e., in the case of DDIM [73],

$$X_{t-1} = \alpha_{t-1} \left(\frac{X_t - \sigma_t \epsilon_\theta(X_t, t, c)}{\alpha_t} \right) + \sigma_{t-1} \epsilon_\theta(X_t, t, c), \quad (1)$$

where ϵ_θ is the *denoiser* neural network such as U-Net [63, 68] or Diffusion Transformer (DiT) [10, 44, 61] and c is user-defined conditioning. In the case of T2I generation $c \in \mathbb{R}^{tok \times d_{tok}}$ is the embedding of a textual prompt, e.g., output of a CLIP [27, 65] or LLM such as T5 [66] where tok and d_{tok} refer to the number of tokens and token embedding dimension, respectively. The objective of ϵ_θ is to facilitate adequate reverse diffusion of X_t with respect to the user-provided conditioning. For example, if c_1 embeds ‘A green dog’ and c_2 embeds ‘A red cat’, the resultant X_{0, c_1} and X_{0, c_2} should yield substantially different images.

However, X_T is randomly sampled, so different initializations will yield qualitatively and quantitatively different results, as prior literature shows [9, 77, 78, 87]. This issue is compounded as ϵ_θ is a large deep neural network that performs iterative inference. Ultimately, this means that while DMs have revolutionized T2I generation, many images will be subpar, leading to wasteful computation.

2.1 Noise-Aware Optimization

Noise-aware optimization is a class of methods which take into account the random stochasticity of X_T to improve DM generation quality in a variety of tasks

such as protein synthesis [34, 72] among others [59, 78, 81]. In the specific context of visual content generation, i.e., T2I DMs, existing literature can generally be subdivided depending on whether fine-tuning of the denoiser DNN ϵ_θ is involved - analogous to the distinction between Post-Training Quantization (PTQ) [26, 40, 42] and Quantization-Aware Training (QAT) [49, 75] methods for DNN bit-precision compression. Naïve PAINE is more like PTQ.

Post-training methodologies apply mutation either to the noise or within the denoiser ϵ_θ itself. For example, InitNO [24] utilize attention map edits [8] during DM inference to alter the generation trajectory and facilitate prompt-adherence [32]. DNO [77] cast X_T as a learnable variable and use reinforcement learning (RL) to train a policy for optimizing it. NoiseQuery [80] collect a finite dataset of high-quality noise samples in an offline fashion and then match the user prompt to the best noise at inference-time rather than sampling X_T . Finally, Golden Noise [90] train a Noise Prompt Network (NPNet) that mutates the initial noise X_T into an optimal ‘golden noise’ X'_T based on the prompt. Although these methods do not require costly fine-tuning of ϵ_θ , they implement a mapping where a single prompt is mapped to a single optimal noise. However, as we show in Section 2.3, the generative performance of a given DM is a statistical distribution with moments conditionally dependent on the user prompt. Thus, in contrast to the existing literature, our proposed Naïve PAINE utilizes sampling from the distribution of generative quality that is conditioned on the prompt.

Finally, in addition to post-training methodologies, there are a number of training [41] or fine-tuning optimization approaches. ReNO [20] and NoiseAR [43] utilize reinforcement learning fine-tuning to optimize the initial noise while HyperNoise [19] combines step-distillation [70] with LLM test-time scaling [55]. These approaches require GPU-intensive fine-tuning the denoiser ϵ_θ and can be restricted in application, i.e., both ReNO and HyperNoise are applicable to step-distilled DMs like SD-Turbo [70] or SANA-Sprint [11]. In contrast, our proposed Naïve PAINE is a model agnostic with plug-and-play integration into existing pipelines for hardware ranging from industrial GPUs to Nvidia DGX Spark units.

2.2 Human Preference Metrics

The past several years have seen the development of a number of benchmarks and tools designed to capture the noisy and subjective human judgment [29, 51, 86] of AI image content with respect to the textual prompt utilized to condition generation. These benchmarks typically utilize some kind of predictor to map a (*prompt, image*) pair to a scalar score value.

The progenitor model for most of these approaches is CLIPScore [27], a common DM evaluation metric where prompt-image pairs are scored by how well the image adheres to the prompt. More recent metrics such as HPSv2 [84], HPSv3 [50], ImageReward [86] and PickScore [38] train a predictor (or fine-tune from CLIPScore) to explicitly model the preference a human judge would express for a given image with respect to the prompt.

Let p be a textual prompt, i.e., ‘A red cat’, and I be an image. Human preference metric predictors first collect a carefully curated dataset of images

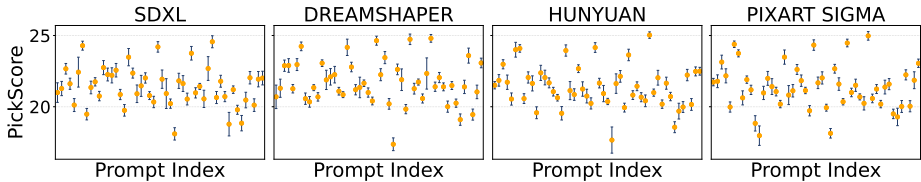


Fig. 1: Measuring the PickScore [38] distribution across several prompts and DMs [10, 44, 47, 63]. Specifically, we select the first 50 training prompts from Golden Noise [90] and generate 20 images per prompt, resetting the random seed prior to the first generation. Then, we plot the PickScore score mean and standard deviation (error bar).

and the human preference rankings for those images. We refer interested readers to specific publications for the exact details behind each metric. Second, these methods train a predictor model ϕ that learns to map prompt-image pairs (p, I) to a *scalar* score $S_{p,I} \in \mathbb{R}$, the numerical representation of the human preference for the image given the prompt. We formally represent this task as follows:

$$S_{p,I} = \phi(p, I). \quad (2)$$

Typically, higher $S_{p,I}$ is better. In an ideal world, we could use a single prompt p to generate several images $\mathcal{I}_p = \{I_1, I_2, \dots, I_N\}$, measure their preference scores $\{S_{p,I_1}, S_{p,I_2}, \dots, S_{p,I_N}\}$ and determine the most preferential image as I_{best} by taking the *argmax* over each image. However, note that ϕ is a predictor that provides accurate, yet imperfect estimations, so I_{best} is not guaranteed to truly be the most preferred image. Rather, a more realistic assumption is that scores lie on some distribution $\mathcal{N}(\mu_{S_p}, \sigma_{S_p})$ and that I_{best} resides in its upper tail.

2.3 Human Preferences and Prompt Influence

We conduct a simple experiment to determine what factors influence the moments, μ_{S_p} and σ_{S_p} , of this distribution. Specifically, we sample 50 prompts from the Pickcapic training set [38] and consider a number of different DMs [4, 10, 12, 44, 85]. For each prompt on each DM, we fix the random seed and then generate 20 images. We then estimate the preference score, and compute the moments of the score population. For each DM, we then plot the mean and standard deviation of the scores based on prompt index.

Figure 1 illustrates our findings. The mean μ_{S_p} of the score distribution highly depends on the prompt p and varies greatly with the prompt index. It is also

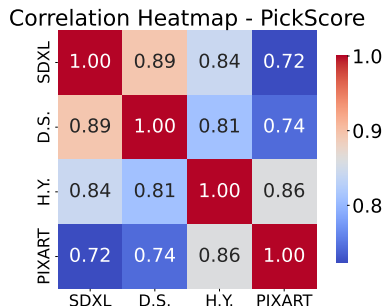


Fig. 2: Pearson Correlation Coefficient (PCC) matrix comparing the mean PickScore for each DM. ‘D.S.’ and ‘H.Y.’ shorthand for [47] and [44].

evident that the standard deviation σ_{S_p} depends on the prompt and noise as the error bars are not consistent across prompts, despite fixing the random seed.

Further, we compare the score distributions across DMs and note that while there are some similarities, i.e., some prompts generally obtain higher or lower preference score, the pattern is noisy. In fact, Figure 2 quantifies the degree to which different score means μ_{S_p} are linearly correlated. This result corroborates [9, 90] and shows that different DMs will excel or produce substandard generation for different subsets of prompts.

Next, we measure to what extent a random initial noise X_T that produces a high score on one prompt p_i will also produce a high score on a different prompt p_j . To this end we compute the Pearson correlation coefficient between two series of scores $\{S_{p_i, I_1}, S_{p_i, I_2}, \dots, S_{p_i, I_N}\}$ and $\{S_{p_j, I_1}, S_{p_j, I_2}, \dots, S_{p_j, I_N}\}$. Figure 3 illustrates our findings, which show that there is very little correlation between choice of noise and preference score across prompts for a given DM.

Overall, the primary insights we draw from these initial background experiments are that the choice of prompt greatly influences the range and distribution of achievable human preference scores more so than the actual DM utilized. Further, the choice of initial noise X_T controls where on the distribution a given image will sit, but the choice of optimal noise must be done on a per-prompt basis. Next, we incorporate these insights into the design of our predictor.

3 Methodology

In this section we introduce Naïve PAINE in detail. Specifically, we describe the PAINE architecture, and how we practically deploy it in a plug-and-play fashion. Finally, we describe how Naïve PAINE provides feedback on prompt generation difficulty. Figure 4 provides a high-level overview of our method.

3.1 Prompt Evaluation Prior to Generation

The PAINE predictor learns to estimate the scalar human preference of a prompt-conditioned image, $S_{p, I}$, from the initial, randomly sampled noise X_T utilized to seed the DM RDP *prior* to committing to costly image generation. Specifically, in the context of DM T2I generation, we first extend Equation 2 to explicitly incorporate the generation process mentioned in Section 2 as follows:

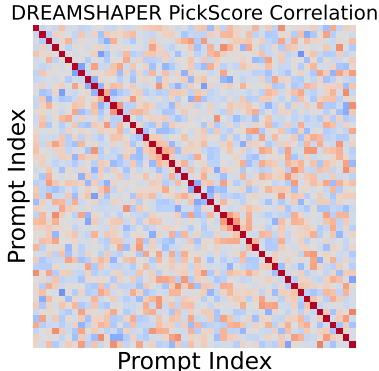


Fig. 3: Pearson Correlation Coefficient (PCC) matrix comparing the mean PickScore across prompts for [47].

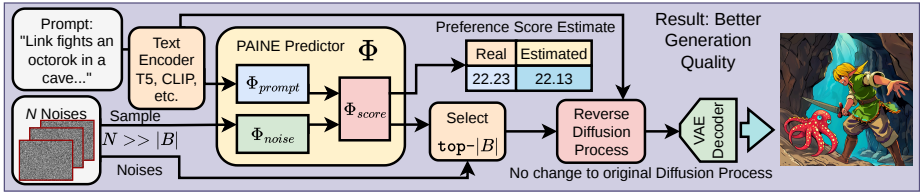


Fig. 4: We augment a DM pipeline with Naïve PAINE which receives the prompt embedding c and N noises as input to estimate the human preference score metric as if each noise were processed into an image. We sort and rank the scores of the N noises and forward the top- $|B|$ noises to the DM for normal generation. Further, score estimations provide feedback to the user on how well the DM can perform on a given prompt. Image from Hunyuan. Scores from our dataset and method on PickScore [38].

$$S_{p,I} = \phi(p, \text{VAE}_D(\text{RDP}_{\epsilon_\theta}(X_T, \text{ENCODE}(p))))), \quad (3)$$

where VAE_D and $\text{RDP}_{\epsilon_\theta}$ represent the VAE decoder [37, 68] utilized to translate denoised latents into image space and the iterative reverse diffusion process from Eq. 1, respectively, while $\text{ENCODE}(p)$ is the DM-specific way of encoding the textual prompt p into its embedding c ; $c = \text{ENCODE}(p)$.

Equation 3 has two inputs: the prompt p and the stochastically sampled initial latent X_T . Per Section 2.3 the user-provided prompt controls the overall score distribution $\mathcal{N}(\mu_{S_p}, \sigma_{S_p})$ while the initial noise determines *where* on the distribution a generated image I will sit. However, we note a key distinction between the *generated image* I and its human preference score $S_{p,I}$. Specifically, an image is a 3D matrix consisting of many elements, i.e., a 1024^2 in RGB space contains over 3M elements, necessitating large computation to *generate*, such as the RDP and compute-intensive denoiser ϵ_θ . In contrast, the score is *just* a single scalar value drawn from a distribution $S_{p,I} \sim \mathcal{N}(\mu_{S_p}, \sigma_{S_p})$ which necessitates smaller computation to *predict* [7, 46, 82, 83]. Thus, we recast the score calculation Eq. 3 in a simpler format,

$$S_{p,I} = \Phi(c, X_T) = \Phi_{\text{score}}(\Phi_{\text{prompt}}(\text{ENCODE}(p)), \Phi_{\text{noise}}(X_T)), \quad (4)$$

where Φ is the PAINE predictor that consists of a prompt-conditioning encoder Φ_{prompt} , noise encoder Φ_{noise} and score predictor Φ_{score} . Whereas existing open-weight human preference predictors ϕ receive the prompt p and generated image I as input, the PAINE predictor receives the DM-specific encoded prompt conditioning c and stochastically-sampled initial latent X_T , $\text{size}(X_T) < \text{size}(I)$ as input to directly predict the scalar preference score.

The intuition and use-case of the PAINE predictor is simple: Given a user-provided prompt p , and desired number of output images $|B|$, the PAINE predictor will first sample $N \gg |B|$ candidate initial noises. Each of the N noises will be fed into the PAINE predictor alongside the prompt encoding c^3 , estimating

³ This incurs no compute overhead since the DM encodes p into c anyway.

a series of scalars $\mathcal{S}_p = \{S_{p,I_1}, S_{p,I_2}, \dots, S_{p,I_N}\}$ which represents the score each noise would receive *if* the costly RDP and denoiser ϵ_θ were invoked to generate an image using that noise. We then sort and rank the candidate noises using their corresponding score estimations in \mathcal{S}_p and proceed to forward the top- $|B|$ candidates for full DM generation into images $\{I_{p,1}, I_{p,2}, \dots, I_{p,|B|}\}$.

This approach differs from existing literature in several ways: *First*, we are considering the scenario where the user may want to generate more than one image per prompt, whereas the frameworks of prior literature [19, 24, 43, 77, 80, 90] target academic benchmark numbers by generally focusing on finding a single optimal noise per prompt. Second, by structuring our predictor around the score distribution $\mathcal{N}(\mu_{S_p}, \sigma_{S_p})$, we more robustly account noise and subjectivity in human preferences in images [29, 51, 86]. Further, we are able to manipulate the components PAINE predictor components in Eq. 4 to provide additional functionality in a Naïve Bayesian [3, 64] manner to provide insight on how well a given DM *can* perform on a given prompt, which we next describe.

3.2 Naïve PAINE: Prompt Generation Performance Estimation

Recall from Section 2.3 that the prompt p primarily influences the score distribution, such that the most/least optimal noise is not consistent across prompts, but rather plays a role in sampling from the score distribution. We train PAINE on a dataset consisting of many $(p, X_T, S_{p,I})$ tuples to predict $S_{p,I}$. In this dataset p is not unique and appears in many tuples, but is matched with different X_T tensors and $S_{p,I}$ scalars. Further details are provided in Section 4.1.

Given this framing, we can further exploit the PAINE architecture to provide additional functionality by predicting μ_{S_p} , the general performance of a given DM denoiser ϵ_θ on the user-provided prompt p . Specifically, we mask Φ_{noise} by zeroing the output *prior* to combining it with the output of Φ_{prompt} and feeding it into Φ_{score} to predict $S_{p,I}$. The intuition is that in the absence of noise information $\Phi_{noise}(X_T)$, Φ_{score} will instead try to approximate μ_{S_p} .

This structure allows us to decompose PAINE such that it functions as a classical Naïve Bayesian [3, 64] predictor, $p(H|E) = p(E|H)p(H)$. Specifically, in the absence of noise information $\Phi_{noise}(X_T)$, PAINE estimates a *prior* $p(H) = \mu_{S_p}$. In this framing the noise information $\Phi_{noise}(X_T)$ acts as the likelihood $p(E|H) = \zeta\sigma_{p,I}$; $\zeta \sim \mathcal{N}(0, 1)$ necessary for us to model the full posterior $p(H|E) = S_{p,I} = \mu_{S_p} + \zeta\sigma_{p,I}$. We articulate the layman explanation of this explanation as ‘What is the average human preference score for this noise given how well the DM can generate given the provided prompt.’ Thus, when embedded into an existing DM pipeline [62], Naïve PAINE not only enables us to perform initial noise optimization, but to manually tweak our prompt to maximize the quality of generated images prior to generation.

4 Results

In this section we evaluate Naïve PAINE on a suite of T2I DMs. Specifically, we enumerate predictor training and pipeline integration in Section 4.1. Next,

Sections 4.2 and 4.3 sweep our evaluation compared to contemporary literature as well as our ability to model preference metric means, respectively. Finally, we provide ablation results in Section 4.4.

4.1 Predictor Architecture, Datasets, Training and Evaluation

We train and evaluate Naïve PAINE on four T2I DMs: Hunyuan-DiT [44], PixArt- Σ [10], DreamShaper-XL-v2-Turbo [47] and SDXL [63] by generating 1024^2 RGB images. For all experiments in this paper, we use the Diffusers [62] DM pipelines unless otherwise indicated.

To train our predictor, we assemble a training set of prompt, noise and score $(p, X_T, S_{p,I})$ tuples. Specifically, we sample 5k random prompts from the Pick-a-Pic [38] training dataset. For each DM, we loop over the prompt set, generating 20 images per prompt with different initial noises. For each prompt-image pair we measure several human preference metrics [27, 84, 86] but primarily rely on PickScore [38] as the target $S_{p,I}$.

The Naïve PAINE predictor architecture Φ consists of three modules. First, the prompt encoder Φ_{prompt} receives the prompt encoding $c = \text{ENCODE}(p)$ and processes it into a vector. To do this, Φ_{prompt} consists of a single transformer layer where we append an additional, learnable token to the end of the sequence prior to the self-attention mechanism. This additional token is passed through the remainder of the transformer block while the original sequence is discarded. Further, we instantiate one distinct Φ_{prompt} per DM text encoder, i.e., one for PixArt- Σ which relies solely on a T5 LLM [66], and two for Hunyuan/SDXL/DreamShaper which all use dual text encoders [65].

The noise encoder Φ_{noise} consists of a simple 4-stage ResNet [25] encoder which gradually downsamples the height and width of the latent X_T while increasing the number of channels. The final layer of Φ_{noise} is an adaptive max pooling layer which compresses the remaining height and width down to 1 for a vector output. Finally, the score encoder Φ_{score} simply concatenates the output of the noise and prompt encoder(s) and then feed them through an MLP to output a scalar prediction.

For training, we split our data 80%/10%/10% into distinct training, validation, and test sets. The overall loss function consists of the Mean Absolute Error (MAE) regression loss and the differentiable Spearman’s Rank Correlation Coefficient (SRCC) from Blondel et al., 2020 [5]. Specifically, the differentiable SRCC loss computes by measuring the soft ranking correlation of ground-truth targets and predictions in a given batch. Naïve PAINE trains for 100 epochs with a batch size of 256 using the Adam [45] optimizer and an initial learning rate of 1×10^{-4} . We find that Naïve PAINE is able to achieve above 0.74 SRCC and below 0.84 MAE on the validation sets for each DM. Further details can be found in the supplementary.

Once trained, our Naïve PAINE predictors integrate into existing DM pipelines as follows: In addition to the prompt p , number of images to generate $|B|$ and other hyperparameters, the user provides the number of initial noises N to sample. After the pipeline encodes the prompt, $c = \text{ENCODE}(p)$, we sample N noises

and estimate their scores $S_{p,I}$. We sort and rank the noises, forwarding only the top- $|B|$ for full generation. Alternatively, given prompt encoding c , Naïve PAINE can also simply estimate the mean preference score μ_{S_p} .

4.2 T2I Evaluation

We evaluate Naïve PAINE on a variety of benchmark prompt sets [38,69,84], human preference predictors ϕ such as HPSv2 [84], HPSv3 [50], ImageReward [86] and PickScore [38]. We also consider the GenEval [22] benchmark which focuses on a DM’s ability to draw numerically specific prompts, e.g., ‘a photo of four zebras’. In terms of baselines we primarily compare to Golden Noise [90] who mutate the initial noise X_T given the prompt and a standard baseline where no initial noise optimization is performed. We also provide some comparisons to NoiseAR [43] who use RL fine-tuning to autoregressively modify the DM generation process. Due to space constraints, we provide additional evaluation results and baseline implementation details in the supplementary.

Human preference benchmarks. Table 1 reports our findings for 64 comparisons across all DM, prompt set and human preference metric ϕ combinations. Naïve PAINE achieves the best performance on more than 30 of these comparisons and the second best performance on more than 20. Further, even though we primarily train our predictor on PickScore, we find that the performance generalizes across other preference metrics, specifically HPSv2 and v3, as well. In terms of performance on specific DMs, we find that our method is generally stronger on newer DiT models like Hunyuan and PixArt- Σ , but is also very competitive on older U-Nets like SDXL and its fine-tune, DreamShaper. Overall, considering the inherent noisiness of human preference metrics [29,51,86], these results demonstrate the generative competitiveness of our proposed method.

Table 2: Overall performance on GenEval [22]. Higher is better. Best in **bold**; second best in *italics*.

Model	Standard	Golden Noise	NoiseAR	Naïve PAINE
Hunyuan	<i>65.78</i>	66.00	65.75	65.20
PixArt- Σ	55.45	55.12	56.16	<i>56.11</i>
DreamShaper	59.26	59.18	59.90	<i>59.38</i>
SDXL	53.61	53.49	55.08	<i>54.05</i>

GenEval. Next, Table 2 provides a simple summary of the overall performance on the GenEval benchmark. Note that a detailed category breakdown is in the supplementary. We observe

that Naïve PAINE achieves high performance on 3 of 4 DMs, second only to NoiseAR which is a costlier fine-tuning-based approach. On Hunyuan, Golden Noise achieves the overall best result but all methods are within 1% of each other overall, which is not the case on the other 3 DMs.

Qualitative Image Comparison. We now consider a qualitative visual comparison. Figure 5 provides some examples and we report additional results in the supplementary. Here, we have a clearer picture of exactly what each method is doing. Specifically, only Naïve PAINE and NoiseAR will substantially change the result from the stochastic baseline, while Golden Noise only makes small edits within the confines of the initial noise. For example, the ‘hypnotoad from

Table 1: T2I Quantitative Comparison on several human preference benchmarks and prompt datasets. Best and second best results in **bold** and *italics*, respectively.

Model	Dataset	Method	HPSv2 (↑)	HPSv3 (↑)	ImageReward (↑)	PickScore (↑)	
Hunyuan	Pick-a-Pic	Standard	29.48	8.06	85.47	21.81	
		Golden Noise	<i>29.94</i>	<i>8.09</i>	<i>87.00</i>	<i>21.85</i>	
		Naïve PAINE	30.77	8.24	89.52	21.86	
	HPDv2	Standard	31.04	10.01	<i>109.27</i>	22.88	
		Golden Noise	<i>31.20</i>	10.12	108.29	<i>22.89</i>	
		Naïve PAINE	32.79	<i>10.02</i>	114.78	23.00	
	HPSv2	Standard	<i>30.06</i>	11.42	106.41	<i>22.58</i>	
		Golden Noise	29.00	11.70	<i>108.25</i>	22.61	
		Naïve PAINE	31.70	<i>11.43</i>	<i>108.42</i>	<i>22.58</i>	
DrawBench	Standard	28.49	<i>9.18</i>	84.45	22.31		
	Golden Noise	<i>29.02</i>	9.66	<i>87.96</i>	22.40		
	Naïve PAINE	30.16	9.10	89.88	<i>22.33</i>		
PixArt- Σ	Pick-a-Pic	Standard	<i>29.83</i>	<i>8.60</i>	<i>81.24</i>	21.90	
		Golden Noise	28.08	7.91	68.13	21.63	
		Naïve PAINE	30.82	8.73	86.02	<i>21.82</i>	
	HPDv2	Standard	<i>30.91</i>	<i>10.53</i>	106.45	<i>22.98</i>	
		Golden Noise	28.97	10.09	98.39	22.82	
		Naïve PAINE	32.71	10.58	<i>106.11</i>	23.01	
	HPSv2	Standard	<i>31.70</i>	<i>11.93</i>	<i>103.21</i>	<i>22.68</i>	
		Golden Noise	28.95	11.56	97.96	22.52	
		Naïve PAINE	31.79	11.96	103.23	22.70	
	DrawBench	Standard	28.54	9.60	<i>73.41</i>	<i>22.33</i>	
		Golden Noise	<i>28.64</i>	8.34	57.95	22.09	
		Naïve PAINE	30.03	<i>9.57</i>	75.60	22.34	
	DreamShaper	Pick-a-Pic	Standard	32.51	<i>10.33</i>	98.06	22.60
			Golden Noise	<i>32.69</i>	10.36	<i>103.91</i>	22.69
			Naïve PAINE	33.27	10.29	106.60	<i>22.64</i>
HPDv2		Standard	<i>33.95</i>	<i>12.38</i>	<i>129.51</i>	23.88	
		Golden Noise	29.85	12.78	133.04	<i>23.62</i>	
		Naïve PAINE	34.85	12.01	119.49	23.59	
HPSv2		Standard	<i>34.39</i>	13.90	121.91	<i>23.42</i>	
		Golden Noise	29.70	14.19	123.66	23.39	
		Naïve PAINE	<i>34.44</i>	<i>13.94</i>	<i>123.24</i>	23.44	
DrawBench		Standard	<i>30.17</i>	11.57	96.37	22.92	
		Golden Noise	29.51	12.17	97.88	23.03	
		Naïve PAINE	31.58	<i>11.70</i>	<i>97.28</i>	<i>22.93</i>	
SDXL		Pick-a-Pic	Standard	28.40	7.10	57.94	21.65
			Golden Noise	<i>28.68</i>	<i>7.20</i>	<i>65.01</i>	21.85
			Naïve PAINE	28.85	7.90	80.86	<i>21.82</i>
	HPDv2	Standard	29.66	8.73	82.66	22.83	
		Golden Noise	<i>29.88</i>	9.07	<i>98.81</i>	22.94	
		Naïve PAINE	31.70	<i>8.95</i>	100.78	<i>22.93</i>	
	HPSv2	Standard	<i>28.69</i>	<i>10.24</i>	85.06	22.52	
		Golden Noise	28.74	10.78	<i>91.07</i>	<i>22.60</i>	
		Naïve PAINE	28.67	10.21	92.37	23.01	
	DrawBench	Standard	26.83	7.88	60.08	22.28	
		Golden Noise	<i>27.14</i>	8.52	67.92	22.38	
		Naïve PAINE	28.66	<i>8.16</i>	<i>66.00</i>	<i>22.31</i>	

Futurama’ does not wear a suit, but does have reptilian eyes. While our method and NoiseAR remove the suit and maintain the proper eye shape, Golden Noise instead preserves the suit and erroneously gives the hypnotoad human-like eyes.

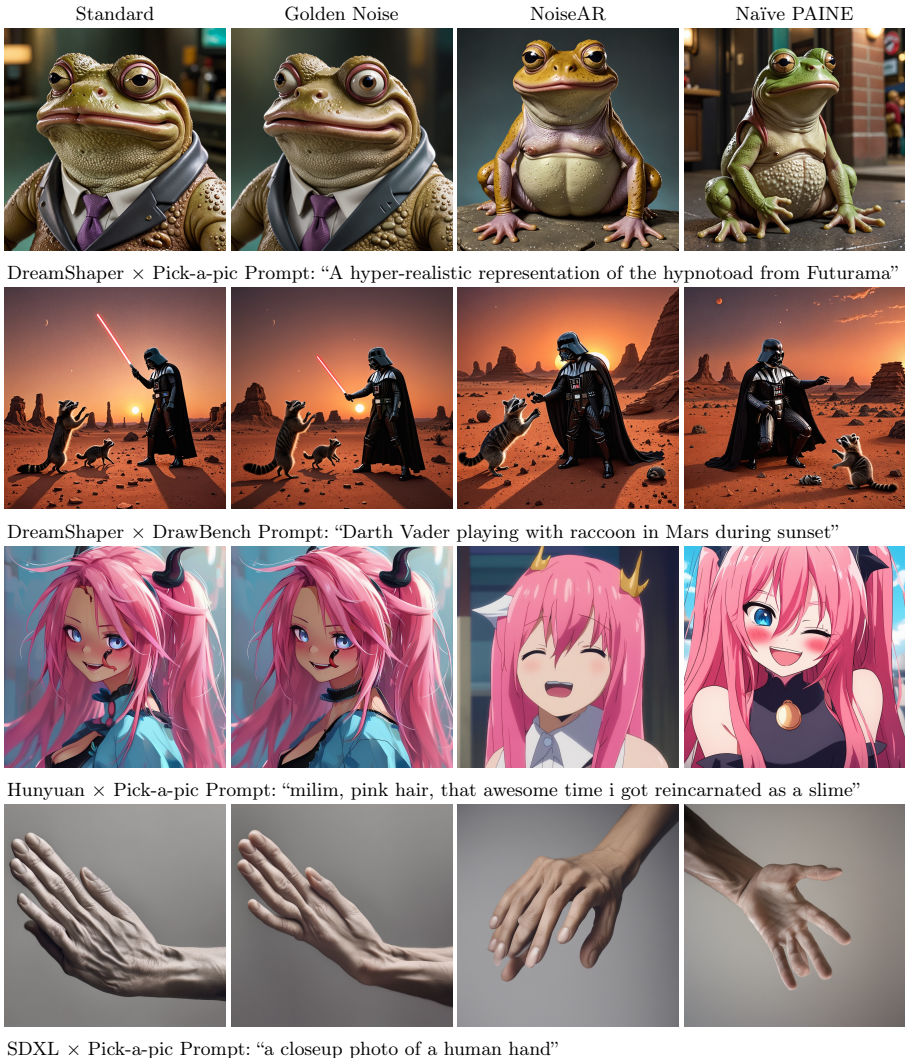


Fig. 5: Qualitative visual examples. DM and prompt details provided. Best viewed in color. We provide further examples in the supplementary materials.

Further, consider the anime image of ‘milim’, where the standard baseline noise produces artifacts on the character’s cheek which Golden Noise does not correct for. Finally, one on-going challenge for DMs, especially older ones like SDXL, has been accurately representing human anatomy [79], especially hands [35, 48, 57]. Despite this hurdle, Naïve PAINE is able to perform initial noise optimization to sufficiently provide a fairly reasonable and realistic image with no extra fingers and minimal distortions.

Hardware Considerations. Finally, we consider the hardware costs of Naïve PAINE as part of a broader, deployed DM pipeline. Due to space constraints

Table 3: Hardware metrics comparing Naïve PAINE to Golden Noise. We measure the parameter count, FLOPs [53], latency on two devices and checkpoint size of the Naïve PAINE predictor compared to Golden Noise’s NPNet.

Model	Method	Params (↓)	FLOPs (↓)	RTX6000 (↓)	DGX Spark (↓)	Ckpt. Size (↓)
Hunyuan	Golden Noise	29.84M	9.29G	8.61ms (1.0x)	16.44ms (1.0x)	119.40MB
	Naïve PAINE	55.12M	9.57G	1.75ms (4.9x)	4.71ms (3.5x)	106.48MB
SDXL/D.S.	Golden Noise	30.47M	9.29G	8.45ms (1.0x)	25.05ms (1.0x)	122.01MB
	Naïve PAINE	55.12M	6.57G	1.03ms (8.2x)	3.24ms (7.7x)	105.48MB

we primarily compare to Golden Noise as the most apples-to-apples method. Table 3 provides hardware measurements for a single inference pass of Naïve PAINE compared to Golden Noise’s NPNet. Specifically, our PAINE predictor consumes more parameters but leverages them towards stronger prompt encoders Φ_{prompt} and is able to perform much faster inference whether on an industrial-grade GPU or DGX Spark. We also have an overall smaller checkpoint size.

However, all measurements in Table 3 consider a single batch size where Naïve PAINE is explicitly a sampling approach where $N \gg |B|$. Thus, we provide a more realistic test in Table 4 where we consider the time it takes to perform initial noise optimization for $|B| = 10$ images on SDXL, which is still one of the most popular DMs for fine-tuning [16, 36, 47, 60]. These results show that Naïve PAINE, despite requiring a larger batch size has noticeably smaller latency cost than Golden Noise.

Table 4: Latency for Golden Noise and Naïve PAINE ($N=100$) to generate $|B| = 10$ optimal noises on an Nvidia RTX 6000 Ada or DGX Spark for SDXL and DreamShaper.

Device	Method	Latency (↓)
RTX6000	Golden Noise	64.46ms
	Naïve PAINE	44.47ms
DGX Spark	Golden Noise	111.97ms
	Naïve PAINE	67.25ms

4.3 Prompt-Aware DM Capability Estimation

We now evaluate the ability of Naïve PAINE to provide accurate feedback on how well a DM can generate images for a given prompt. Following Section 3.2, this is done by masking the noise encoder Φ_{noise} and only relying on Φ_{prompt} to predict μ_{S_p} instead of $S_{p,I}$. Specifically, we use a special dataloader where all images in a batch have the same prompt encoding, but a different noise. From the batch we compute a single ground-truth target as the average of all single score targets μ_{S_p} , and perform one inference pass on just the prompt encoding which is consistent throughout the batch. We perform this task on our pretrained predictors for each DM using their specific prompt-noise validation set.

Table 5 reports our findings. This table includes the ground-truth score distributions for reference. As we can see, in terms of ranking performance (SRCC) and regression error (MAE/MAPE), our method is able to provide competent feedback to an end-user on DM generation capacity for a given prompt. Specifically, we note that Naïve PAINE achieves less than 4% MAPE on all four DMs and achieve over 0.7 SRCC on three of four DMs.

Table 5: Prompt-only prediction results for all four DMs. We enumerate the distribution of Pick-a-Pic prompt scores in the validation dataset. Next, we report predictor performance metrics when Naïve PAINE predicts the score mean μ_{S_p} for a given prompt using only the prompt embedding as a prior.

Model	Score Distribution	Score Range	SRCC (\uparrow)	MAE (\downarrow)	MAPE (\downarrow)
Hunyuan	$\mathcal{N}(21.72, 1.43)$	[19.44, 26.71]	0.7414	0.7643	3.61%
PixArt- Σ	$\mathcal{N}(21.74, 1.47)$	[18.26, 25.65]	0.6785	0.8388	3.88%
DreamShaper	$\mathcal{N}(22.04, 1.40)$	[18.46, 25.84]	0.7450	0.7097	3.26%
SDXL	$\mathcal{N}(21.76, 1.31)$	[18.76, 25.96]	0.7416	0.6687	3.08%

4.4 Ablation Studies

We ablate the sensitivity of Naïve PAINE to different human preference metrics. Specifically, we vary the choice of human preference metric utilized to train the predictor, from HPSv2 [84] to ImageReward [86] to PickScore [38] for Naïve PAINE on SDXL. We then observe the effect on T2I quality by using these predictors to generate images using prompts from the PickScore test set.

Figure 6 illustrates the result. First, we observe that while both HPSv2 and ImageReward, when used as a predictor metric, achieve slightly superior HPSv2 evaluation performance compared to PickScore, they both fall short of it on HPSv3 [50] and ImageReward evaluation performance. Ironically, when we use ImageReward scores to train Naïve PAINE, it provides the worst ImageReward benchmark performance. Further, using PickScore to train the predictor also yields the best PickScore evaluative performance. This finding is one example of why we select PickScore to generate results in Section 4.2 as we ran many trials and generally found that it achieves better overall performance in comparison to HPSv2 or ImageReward, and compared to other baselines. We provide additional ablations and examples in the supplementary materials.

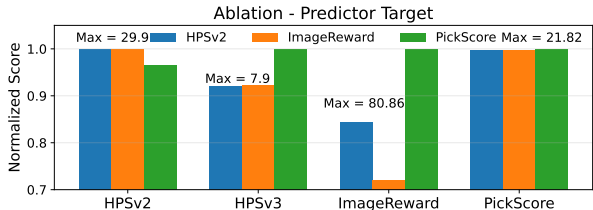


Fig. 6: Comparing the performance of Naïve PAINE on the PickScore test set when we vary the choice of preference metric utilized to train the predictor. Values normalized based on the maximum (annotated).

5 Conclusions and Future Work

We propose Naïve PAINE, a simple and lightweight method for initial noise optimization on Text-to-Image (T2I) Diffusion Models (DM). Specifically, Naïve PAINE achieves superior generative quality whilst also providing feedback on DM generative ability for a user-provided prompt. Specifically, our method leverages advances in estimating human preferences from prompt-image pairs to directly estimate a human preference score using prompt encodings and

stochastically-sampled initial noises. Naïve PAINE achieves superior qualitative and quantitative results compared to existing fine-tuning-free approaches whilst incurring a smaller hardware latency if integrated into an existing DM pipeline. Future directions of this line of research include:

1. Extending Naïve PAINE to other generative models like in Text-to-Video (T2V) DMs or Autoregressive image models.
2. Integration of DM components with sparse, open-source data, such as low-rank adapters.
3. Incorporating other user-provided setting such as the choice of sampler, scheduler, etc., into the predictor.

References

1. AUTOMATIC1111: Stable diffusion webui. <https://github.com/AUTOMATIC1111/stable-diffusion-webui> (2022)
2. Bai, L., Shao, S., Zhou, Z., Qi, Z., Xu, Z., Xiong, H., Xie, Z.: Zigzag diffusion sampling: Diffusion models can self-improve via self-reflection. arXiv preprint arXiv:2412.10891 (2024)
3. Bishop, C.M., Nasrabadi, N.M.: Pattern recognition and machine learning, vol. 4. Springer (2006)
4. Black Forest Labs: Flux. <https://github.com/black-forest-labs/flux> (2024)
5. Blondel, M., Teboul, O., Berthet, Q., Djolonga, J.: Fast differentiable sorting and ranking. In: International Conference on Machine Learning. pp. 950–959. PMLR (2020)
6. Cai, H., Cao, S., Du, R., Gao, P., Hoi, S., Hou, Z., Huang, S., Jiang, D., Jin, X., Li, L., et al.: Z-image: An efficient image generation foundation model with single-stream diffusion transformer. arXiv preprint arXiv:2511.22699 (2025)
7. canals: Now and next for ai-capable smartphones. Tech. rep., A Canals Special Report (05 2024)
8. Chefer, H., Alaluf, Y., Vinker, Y., Wolf, L., Cohen-Or, D.: Attend-and-excite: Attention-based semantic guidance for text-to-image diffusion models. *ACM transactions on Graphics (TOG)* **42**(4), 1–10 (2023)
9. Chen, C., Yang, L., Yang, X., Chen, L., He, G., Wang, C., Li, Y.: Find: Fine-tuning initial noise distribution with policy optimization for diffusion models. In: Proceedings of the 32nd ACM International Conference on Multimedia. pp. 6735–6744 (2024)
10. Chen, J., Ge, C., Xie, E., Wu, Y., Yao, L., Ren, X., Wang, Z., Luo, P., Lu, H., Li, Z.: PixArt- Σ : Weak-to-strong training of diffusion transformer for 4k text-to-image generation. In: European Conference on Computer Vision. pp. 74–91. Springer (2025)
11. Chen, J., Xue, S., Zhao, Y., Yu, J., Paul, S., Chen, J., Cai, H., Han, S., Xie, E.: Sana-sprint: One-step diffusion with continuous-time consistency distillation. In: Proceedings of the IEEE/CVF International Conference on Computer Vision. pp. 16185–16195 (2025)
12. Chen, J., Yu, J., Ge, C., Yao, L., Xie, E., Wang, Z., Kwok, J.T., Luo, P., Lu, H., Li, Z.: Pixart- α : Fast training of diffusion transformer for photorealistic text-to-image synthesis. In: The Twelfth International Conference on Learning Representations, ICLR 2024, Vienna, Austria, May 7-11, 2024. OpenReview.net (2024), <https://openreview.net/forum?id=eAKmQPe3m1>

13. Civitai: Civitai: The Generative AI Community Hub. [urlhttps://civitai.com](https://civitai.com) (2026), accessed on January 27, 2026
14. Cohen, P.: Harold cohen and aaron. *Ai Magazine* **37**(4), 63–66 (2016)
15. Contributors, C.: Comfyui: A node-based gui for stable diffusion (2025), <https://github.com/Comfy-Org/ComfyUI>
16. Cyberdelia: CyberRealistic Pony - | Stable Diffusion XL Checkpoint | Civitai — [civitai.com](https://civitai.com/models/443821/cyberrealistic-pony). <https://civitai.com/models/443821/cyberrealistic-pony> (2026), [Accessed 02-03-2026]
17. Delfabbro, P., King, D., Parke, J.: The complex nature of human operant gambling behaviour involving slot games: Structural characteristics, verbal rules and motivation. *Addictive Behaviors* **137**, 107540 (2023)
18. Esser, P., Kulal, S., Blattmann, A., Entezari, R., Müller, J., Saini, H., Levi, Y., Lorenz, D., Sauer, A., Boesel, F., Podell, D., Dockhorn, T., English, Z., Rombach, R.: Scaling rectified flow transformers for high-resolution image synthesis. In: Forty-first International Conference on Machine Learning, ICML 2024, Vienna, Austria, July 21-27, 2024. OpenReview.net (2024), <https://openreview.net/forum?id=FPnUhsQJ5B>
19. Eyring, L., Karthik, S., Dosovitskiy, A., Ruiz, N., Akata, Z.: Noise hypernetworks: Amortizing test-time compute in diffusion models. arXiv preprint arXiv:2508.09968 (2025)
20. Eyring, L., Karthik, S., Roth, K., Dosovitskiy, A., Akata, Z.: Reno: Enhancing one-step text-to-image models through reward-based noise optimization. *Advances in Neural Information Processing Systems* **37**, 125487–125519 (2024)
21. Ferrari, M.A., Limbrick-Oldfield, E.H., Clark, L.: Behavioral analysis of habit formation in modern slot machine gambling. *International Gambling Studies* **22**(2), 317–336 (2022)
22. Ghosh, D., Hajishirzi, H., Schmidt, L.: Geneval: An object-focused framework for evaluating text-to-image alignment. *Advances in Neural Information Processing Systems* **36**, 52132–52152 (2023)
23. Goodfellow, I., Pouget-Abadie, J., Mirza, M., Xu, B., Warde-Farley, D., Ozair, S., Courville, A., Bengio, Y.: Generative adversarial nets. In: *Advances in neural information processing systems*. pp. 2672–2680 (2014)
24. Guo, X., Liu, J., Cui, M., Li, J., Yang, H., Huang, D.: Initno: Boosting text-to-image diffusion models via initial noise optimization. In: *Proceedings of the IEEE/CVF Conference on Computer Vision and Pattern Recognition*. pp. 9380–9389 (2024)
25. He, K., Zhang, X., Ren, S., Sun, J.: Deep residual learning for image recognition. In: *Proceedings of the IEEE conference on computer vision and pattern recognition*. pp. 770–778 (2016)
26. He, Y., Liu, L., Liu, J., Wu, W., Zhou, H., Zhuang, B.: Ptqd: Accurate post-training quantization for diffusion models. *Advances in Neural Information Processing Systems* **36** (2024)
27. Hessel, J., Holtzman, A., Forbes, M., Le Bras, R., Choi, Y.: CLIPScore: A reference-free evaluation metric for image captioning. In: Moens, M.F., Huang, X., Specia, L., Yih, S.W.t. (eds.) *Proceedings of the 2021 Conference on Empirical Methods in Natural Language Processing*. pp. 7514–7528. Association for Computational Linguistics, Online and Punta Cana, Dominican Republic (Nov 2021). <https://doi.org/10.18653/v1/2021.emnlp-main.595>, <https://aclanthology.org/2021.emnlp-main.595/>
28. Ho, J., Jain, A., Abbeel, P.: Denoising diffusion probabilistic models. *Advances in neural information processing systems* **33**, 6840–6851 (2020)

29. Jaramillo, D.: Radiologists and their noise: variability in human judgment, fallibility, and strategies to improve accuracy (2022)
30. Jiang, L., Chen, R., Gao, C., Niu, D.: Raise: Requirement-adaptive evolutionary refinement for training-free text-to-image alignment (2026), <https://arxiv.org/abs/2603.00483>
31. Jiang, L., Hassanpour, N., Salameh, M., Samadi, M., He, J., Sun, F., Niu, D.: Pixelman: Consistent object editing with diffusion models via pixel manipulation and generation. In: Proceedings of the AAAI Conference on Artificial Intelligence. vol. 39, pp. 4012–4020 (2025)
32. Jiang, L., Hassanpour, N., Salameh, M., Samadi, M., He, J., Sun, F., Niu, D.: Pixelman: Consistent object editing with diffusion models via pixel manipulation and generation. In: Proceedings of the AAAI Conference on Artificial Intelligence (2025)
33. Jiang, L., Hassanpour, N., Salameh, M., Singamsetti, M.S., Sun, F., Lu, W., Niu, D.: Frap: Faithful and realistic text-to-image generation with adaptive prompt weighting. arXiv preprint arXiv:2408.11706 (2024)
34. Kalaivanan, A., Zhao, Z., Sjölund, J., Lindsten, F.: Ess-flow: Training-free guidance of flow-based models as inference in source space. arXiv preprint arXiv:2510.05849 (2025)
35. Kamali, N., Nakamura, K., Kumar, A., Chatzimparmpas, A., Hullman, J., Groh, M.: Characterizing photorealism and artifacts in diffusion model-generated images. In: Proceedings of the 2025 CHI Conference on Human Factors in Computing Systems. pp. 1–26 (2025)
36. KandooAI: Juggernaut XL - Ragnarok_by_RunDiffusion | Stable Diffusion XL Checkpoint | Civitai — civitai.com. <https://civitai.com/models/133005/juggernaut-xl> (2025), [Accessed 27-01-2026]
37. Kingma, D.P., Welling, M.: An introduction to variational autoencoders. *Found. Trends Mach. Learn.* **12**(4), 307–392 (2019). <https://doi.org/10.1561/22000000056>, <https://doi.org/10.1561/22000000056>
38. Kirstain, Y., Polyak, A., Singer, U., Matiana, S., Penna, J., Levy, O.: Pick-a-pic: An open dataset of user preferences for text-to-image generation. *Advances in neural information processing systems* **36**, 36652–36663 (2023)
39. Koerner, B.I.: Russians engineer a brilliant slot machine cheat—and casinos have no fix. *WIRED* (Aug 2017), https://www.realclearinvestigations.com/links/2017/08/09/meet_a_russian_casino_hacker_104376.html, feature on a St. Petersburg group predicting outcomes by modeling slot PRNG temporal state
40. Li, X., Liu, Y., Lian, L., Yang, H., Dong, Z., Kang, D., Zhang, S., Keutzer, K.: Q-diffusion: Quantizing diffusion models. In: Proceedings of the IEEE/CVF International Conference on Computer Vision. pp. 17535–17545 (2023)
41. Li, Y., Jiang, H., Kodaira, A., Tomizuka, M., Keutzer, K., Xu, C.: Immiscible diffusion: Accelerating diffusion training with noise assignment. *Advances in neural information processing systems* **37**, 90198–90225 (2024)
42. Li, Y., Gong, R., Tan, X., Yang, Y., Hu, P., Zhang, Q., Yu, F., Wang, W., Gu, S.: BRECCQ: pushing the limit of post-training quantization by block reconstruction. In: 9th International Conference on Learning Representations, ICLR 2021, Virtual Event, Austria, May 3-7, 2021. OpenReview.net (2021), <https://openreview.net/forum?id=P0Wv6hDd9XH>
43. Li, Z., Liu, X., Zhang, X., Tan, P., Shum, H.Y.: Noisear: Autoregressing initial noise prior for diffusion models. arXiv preprint arXiv:2506.01337 (2025)

44. Li, Z., Zhang, J., Lin, Q., Xiong, J., Long, Y., Deng, X., Zhang, Y., Liu, X., Huang, M., Xiao, Z., Chen, D., He, J., Li, J., Li, W., Zhang, C., Quan, R., Lu, J., Huang, J., Yuan, X., Zheng, X., Li, Y., Zhang, J., Zhang, C., Chen, M., Liu, J., Fang, Z., Wang, W., Xue, J., Tao, Y., Zhu, J., Liu, K., Lin, S., Sun, Y., Li, Y., Wang, D., Chen, M., Hu, Z., Xiao, X., Chen, Y., Liu, Y., Liu, W., Wang, D., Yang, Y., Jiang, J., Lu, Q.: Hunyuan-dit: A powerful multi-resolution diffusion transformer with fine-grained chinese understanding (2024)
45. Loshchilov, I., Hutter, F.: Decoupled weight decay regularization. In: 7th International Conference on Learning Representations, ICLR 2019, New Orleans, LA, USA, May 6-9, 2019. OpenReview.net (2019), <https://openreview.net/forum?id=Bkg6RiCqY7>
46. Lu, S., Hu, Y., Wang, P., Han, Y., Tan, J., Li, J., Yang, S., Liu, J.: Pinat: A permutation invariance augmented transformer for nas predictor. In: Proceedings of the AAAI Conference on Artificial Intelligence (AAAI) (2023)
47. Lykon: Dreamshaper - stable diffusion fine-tune. <https://civitai.com/models/4384/dreamshaper> (2023)
48. Ma, L., Cao, K., Liang, H., Lin, J., Li, Z., Liu, Y., Zhang, J., Zhang, W., Cui, B.: Evaluating and predicting distorted human body parts for generated images. arXiv preprint arXiv:2503.00811 (2025)
49. Ma, S., Wang, H., Ma, L., Wang, L., Wang, W., Huang, S., Dong, L., Wang, R., Xue, J., Wei, F.: The era of 1-bit llms: All large language models are in 1.58 bits. arXiv preprint arXiv:2402.17764 (2024)
50. Ma, Y., Wu, X., Sun, K., Li, H.: Hpsv3: Towards wide-spectrum human preference score. In: Proceedings of the IEEE/CVF International Conference on Computer Vision. pp. 15086–15095 (2025)
51. Mance, J.: Noise: A flaw in human judgment (2022)
52. Mills, K.G., Han, F.X., Salameh, M., Lu, S., Zhou, C., He, J., Sun, F., Niu, D.: Building optimal neural architectures using interpretable knowledge. In: CVPR (2024)
53. Mills, K.G., Niu, D., Salameh, M., Qiu, W., Han, F.X., Liu, P., Zhang, J., Lu, W., Jui, S.: Aio-p: Expanding neural performance predictors beyond image classification. Proceedings of the AAAI Conference on Artificial Intelligence **37**(8), 9180–9189 (06 2023). <https://doi.org/10.1609/aaai.v37i8.26101>, <https://ojs.aaai.org/index.php/AAAI/article/view/26101>
54. Mills, K.G., Salameh, M., Chen, R., Hassanpour, Negar Lu, W., Niu, D.: Qua²sedimo: Quantifiable quantization sensitivity of diffusion models. In: AAAI (2025)
55. Muennighoff, N., Yang, Z., Shi, W., Li, X.L., Fei-Fei, L., Hajishirzi, H., Zettlemoyer, L., Liang, P., Candès, E., Hashimoto, T.B.: s1: Simple test-time scaling. In: Proceedings of the 2025 Conference on Empirical Methods in Natural Language Processing. pp. 20286–20332 (2025)
56. Nake, F.: There should be no computer-art. Page, Bulletin of the Computer Arts Society (18), 1–2 (1971)
57. Narasimhaswamy, S., Bhattacharya, U., Chen, X., Dasgupta, I., Mitra, S., Hoai, M.: Handdiffuser: Text-to-image generation with realistic hand appearances. In: Proceedings of the IEEE/CVF Conference on Computer Vision and Pattern Recognition. pp. 2468–2479 (2024)
58. Nees, G.: Generative Computergraphik. Ph.D. thesis, University of Stuttgart (1969), https://archive.org/details/generative_computergraphik

59. Om, K., Sim, K., Yun, T., Kang, H., Park, J.: Posterior inference in latent space for scalable constrained black-box optimization. arXiv preprint arXiv:2507.00480 (2025)
60. ONOMAAI: Illustrious XL 2.0 - v2.0 | Illustrious Checkpoint | Civitai — civitai.com. <https://civitai.com/models/1369089/illustrious-xl-20> (2025), [Accessed 27-01-2026]
61. Peebles, W., Xie, S.: Scalable diffusion models with transformers. In: Proceedings of the IEEE/CVF International Conference on Computer Vision. pp. 4195–4205 (2023)
62. von Platen, P., Patil, S., Lozhkov, A., Cuenca, P., Lambert, N., Rasul, K., Davaadorj, M., Nair, D., Paul, S., Berman, W., Xu, Y., Liu, S., Wolf, T.: Diffusers: State-of-the-art diffusion models. <https://github.com/huggingface/diffusers> (2022)
63. Podell, D., English, Z., Lacey, K., Blattmann, A., Dockhorn, T., Müller, J., Penna, J., Rombach, R.: SDXL: improving latent diffusion models for high-resolution image synthesis. In: The Twelfth International Conference on Learning Representations, ICLR 2024, Vienna, Austria, May 7-11, 2024. OpenReview.net (2024), <https://openreview.net/forum?id=di52zR8xgf>
64. Provost, F., Fawcett, T.: Data Science for Business: What you need to know about data mining and data-analytic thinking. " O'Reilly Media, Inc." (2013)
65. Radford, A., Kim, J.W., Hallacy, C., Ramesh, A., Goh, G., Agarwal, S., Sastry, G., Askell, A., Mishkin, P., Clark, J., et al.: Learning transferable visual models from natural language supervision. In: International conference on machine learning. pp. 8748–8763. Pmlr (2021)
66. Raffel, C., Shazeer, N., Roberts, A., Lee, K., Narang, S., Matena, M., Zhou, Y., Li, W., Liu, P.J.: Exploring the limits of transfer learning with a unified text-to-text transformer. *Journal of machine learning research* **21**(140), 1–67 (2020)
67. Ramesh, A., Pavlov, M., Goh, G., Gray, S., Voss, C., Radford, A., Chen, M., Sutskever, I.: Zero-shot text-to-image generation. In: International conference on machine learning. pp. 8821–8831. Pmlr (2021)
68. Rombach, R., Blattmann, A., Lorenz, D., Esser, P., Ommer, B.: High-resolution image synthesis with latent diffusion models. In: CVPR (2022)
69. Saharia, C., Chan, W., Saxena, S., Li, L., Whang, J., Denton, E.L., Ghasemipour, K., Gontijo Lopes, R., Karagol Ayan, B., Salimans, T., et al.: Photorealistic text-to-image diffusion models with deep language understanding. *Advances in neural information processing systems* **35**, 36479–36494 (2022)
70. Sauer, A., Lorenz, D., Blattmann, A., Rombach, R.: Adversarial diffusion distillation. arXiv preprint arXiv:2311.17042 (2023)
71. Schneier, B.: Predicting a slot machine’s prng (Feb 2017), https://www.schneier.com/blog/archives/2017/02/predicting_a_sl.html, security commentary on the 2017 WIRED report about a Russian group reverse-engineering a Novomatic slot PRNG
72. Smith, H.D., Diamant, N.L., Trippe, B.L.: Calibrating generative models. arXiv preprint arXiv:2510.10020 (2025)
73. Song, J., Meng, C., Ermon, S.: Denoising diffusion implicit models. arXiv preprint arXiv:2010.02502 (2020)
74. Song, Y., Dhariwal, P., Chen, M., Sutskever, I.: Consistency models. arXiv preprint arXiv:2303.01469 (2023)
75. Sui, Y., Li, Y., Kag, A., Idelbayev, Y., Cao, J., Hu, J., Sagar, D., Yuan, B., Tulyakov, S., Ren, J.: Bitsfusion: 1.99 bits weight quantization of diffusion model. *Advances in Neural Information Processing Systems* **37** (2024)

76. Tang, H., Wu, Y., Yang, S., Xie, E., Chen, J., Chen, J., Zhang, Z., Cai, H., Lu, Y., Han, S.: Hart: Efficient visual generation with hybrid autoregressive transformer. arXiv preprint arXiv:2410.10812 (2024)
77. Tang, Z., Peng, J., Tang, J., Hong, M., Wang, F., Chang, T.H.: Inference-time alignment of diffusion models with direct noise optimization. arXiv preprint arXiv:2405.18881 (2024)
78. Venkatraman, S., Hasan, M., Kim, M., Scimeca, L., Sendera, M., Bengio, Y., Berseth, G., Malkin, N.: Outsourced diffusion sampling: Efficient posterior inference in latent spaces of generative models. arXiv preprint arXiv:2502.06999 (2025)
79. Wang, J., Sun, Z., Tan, Z., Chen, X., Chen, W., Li, H., Zhang, C., Song, Y.: Towards effective usage of human-centric priors in diffusion models for text-based human image generation. In: Proceedings of the IEEE/CVF Conference on Computer Vision and Pattern Recognition. pp. 8446–8455 (2024)
80. Wang, R., Huang, H., Zhu, Y., Russakovsky, O., Wu, Y.: The silent assistant: Noisequery as implicit guidance for goal-driven image generation. In: Proceedings of the IEEE/CVF International Conference on Computer Vision. pp. 17618–17628 (2025)
81. Wang, Z., Harting, A., Barreau, M., Zavlanos, M.M., Johansson, K.H.: Source-guided flow matching. arXiv preprint arXiv:2508.14807 (2025)
82. Wen, W., Liu, H., Chen, Y., Li, H., Bender, G., Kindermans, P.J.: Neural predictor for neural architecture search. In: European Conference on Computer Vision. pp. 660–676. Springer (2020)
83. White, C., Zela, A., Ru, R., Liu, Y., Hutter, F.: How powerful are performance predictors in neural architecture search? NeurIPS (2021)
84. Wu, X., Hao, Y., Sun, K., Chen, Y., Zhu, F., Zhao, R., Li, H.: Human preference score v2: A solid benchmark for evaluating human preferences of text-to-image synthesis. arXiv preprint arXiv:2306.09341 (2023)
85. Xie, E., Chen, J., Chen, J., Cai, H., Tang, H., Lin, Y., Zhang, Z., Li, M., Zhu, L., Lu, Y., Han, S.: SANA: efficient high-resolution text-to-image synthesis with linear diffusion transformers. In: The Thirteenth International Conference on Learning Representations, ICLR 2025, Singapore, April 24–28, 2025. OpenReview.net (2025), <https://openreview.net/forum?id=N80j1XhtYZ>
86. Xu, J., Liu, X., Wu, Y., Tong, Y., Li, Q., Ding, M., Tang, J., Dong, Y.: Imagereward: Learning and evaluating human preferences for text-to-image generation. Advances in Neural Information Processing Systems **36**, 15903–15935 (2023)
87. Xu, K., Zhang, L., Shi, J.: Good seed makes a good crop: Discovering secret seeds in text-to-image diffusion models. In: 2025 IEEE/CVF Winter Conference on Applications of Computer Vision (WACV). pp. 3024–3034. IEEE (2025)
88. Xu, Z., Wang, Y., Yang, X., Wang, L., Luo, W., Zhang, K., Hu, B., Zhang, M.: Comfyui-r1: Exploring reasoning models for workflow generation. arXiv preprint arXiv:2506.09790 (2025)
89. Zhang, L., Rao, A., Agrawala, M.: Adding conditional control to text-to-image diffusion models. In: Proceedings of the IEEE/CVF international conference on computer vision. pp. 3836–3847 (2023)
90. Zhou, Z., Shao, S., Bai, L., Zhang, S., Xu, Z., Han, B., Xie, Z.: Golden noise for diffusion models: A learning framework. In: Proceedings of the IEEE/CVF International Conference on Computer Vision. pp. 17688–17697 (2025)

Supplementary Materials

We provide additional information and materials to support the main manuscript. Specifically, we provide additional experimental setup and execution details, extensive quantitative evaluation results for NoiseAR [43] and GenEval [22], additional results comparing to the RLHF-driven [19] on the few-step SANA-Sprint [11], further ablation studies and additional qualitative image samples.

A Additional Implementation Details

We provide further details on the implementation of Naïve PAINE. Further, we discuss how we conduct experiments with baseline methods.

A.1 Training Details

Dataset. We train one Naïve PAINE predictor per DM. For each DM we sample 5k prompts from the Pick-a-Pic [38] training set and generate 20 images per prompt, each seeded with an independent Gaussian noise tensor, yielding 100k $(p, X_T, S_{s,I})$ tuples per DM. All preference scores are computed before training begins. Prompt embeddings are pre-encoded with the DM’s native text encoder and cached as `.pt` files; noise tensors are likewise stored on disk. We split data by prompt into 80%/10%/10% into distinct training, validation, and test sets. Target scores are z-score normalized $z = (x - \mu)/\sigma$ using the training-split mean and standard deviation, which we store alongside the checkpoint for inference-time de-normalization.

Grouped Batching. We implement a custom `PromptGroupedBatchSampler` that groups $k = 12$ prompts per batch. Each prompt has ~ 20 noise samples and each batch contains ~ 240 samples spanning 12 prompts.

Loss function. We implement a mixed regression/ranking loss function:

$$\mathcal{L} = \mathcal{L}_{\text{MAE}} + \mathcal{L}_{\text{SRCC}}, \quad (5)$$

where \mathcal{L}_{MAE} is the mean absolute error between the predicted and ground-truth (normalized) scores. $\mathcal{L}_{\text{SRCC}}$ is the differentiable Spearman Rank Correlation Coefficient loss from Blondel *et al.* [5], computed *per prompt group* and averaged over groups within the batch (regularization strength = 10^{-2}). Following [52,54], the ranking SRCC loss encourages the model to rank noises correctly within each prompt rather than minimizing global regression error.

Optimizer and scheduler. We use AdamW [45] with learning rate 10^{-4} and weight decay 10^{-8} . Gradients are clipped to a maximum ℓ_2 -norm of 1.0. The learning rate is halved (`factor=0.5`) if validation SRCC does not improve for 5 consecutive epochs (`ReduceLROnPlateau`). We train for up to 100 epochs with early stopping: training is halted if validation SRCC does not improve for 15 consecutive epochs. The checkpoint with the highest validation SRCC is selected as the final model.

Evaluation metrics. During training we monitor two metrics:

- **SRCC**: global Spearman rank correlation between predicted and ground-truth scores across all validation samples. computed *per prompt* and macro-averaged. Targets are min-max scaled to $[0, 5]$ before gain computation (exponential gain, `exp2`).
- **MAE**: mean absolute error on raw (de-normalized) score values.

Table 6 provides some quantitative results for the PAINE predictor on the different DMs we consider in the main manuscript. Overall, we see that our method obtains competent MAE and SRCC on the validation sets.

Table 6: Naïve PAINE predictor performance on the validation set for each DM, trained with PickScore as target.

DM	Val SRCC (\uparrow)	Val MAE (\downarrow)
Hunyuan-DiT	0.7416	0.8322
PixArt- Σ	0.8020	0.6704
DreamShaper	0.8400	0.5775
SDXL	0.8745	0.4597

A.2 Baseline Implementation

Standard baseline. We simply use the vanilla DM pipeline from HuggingFace Diffusers [62] without any initial noise optimization. For each prompt, we reset the random seed generator using the numerical index of the prompt, a technique that is shared across Naïve PAINE and the other baselines.

Golden Noise [90]. We use the official open-source NPNet checkpoints. For PixArt- Σ , which borrows the $X_T \in \mathbb{R}^{4 \times 128 \times 128}$ for 1024² image latent space from SDXL, but has no provided checkpoint, we apply the SDXL weights and text encoder as a proxy.

NoiseAR [43]. We use the open-source pretrained weights. The checkpoint for both SDXL and DreamShaper is shared across both DMs; for Hunyuan-DiT the DiT-specific checkpoint is used. For PixArt- Σ we reuse the SDXL weights. Image generation follows the same settings as Golden Noise above.

B Extended Quantitative Results

We substantiate our background preliminary results on the impact of a prompt on preference score distribution. We also upon the quantitative results comparing Naïve PAINE to contemporary baseline approaches on a variety of benchmarks.

Extended prompt score distributions. Figure 7 extends Figure 1 across different human preference metrics for the same DMs. Specifically, we provide additional results on HPSv2 [84], ImageReward [86] and CLIPScore [27]. As we can see, the distribution of scores by mean $\mu_{S_{p,I}}$ and standard deviation $\sigma_{S_{p,I}}$ primarily depend on the prompt p across different DMs and preference metrics. Further, while some prompts stand out as easier or harder to achieve a high score for than others, by visual inspection the exact distributions vary across DM with no perfect correlation.

The most interesting empirical finding of Figure 7 is how much variance there is within ImageReward. Although the scales of different human preference metrics are not directly comparable, we can visually observe a much larger average variance in score distributions compared to other methods, especially on the U-Net DMs, SDXL and its fine-tune, DreamShaper.

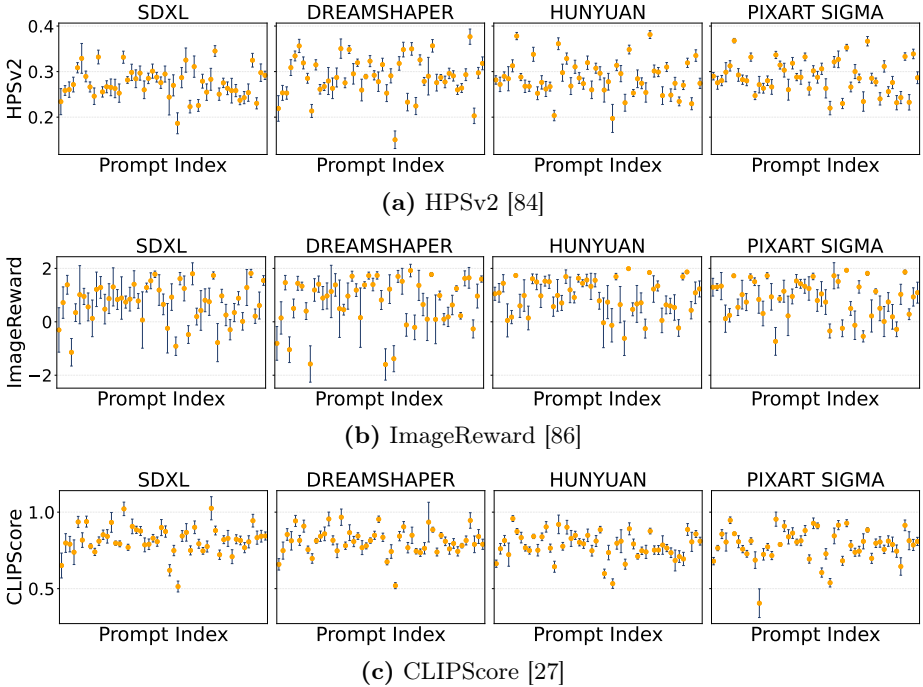


Fig. 7: Extending Figure 1 to different human preference/prompt adherence metrics.

Additional T2I metrics. Table 7 provides additional quantitative results on prompt datasets like Pick-a-Pic or DrawBench and various human preference metrics like HPSv2/v3. Specifically, we compare Naïve PAINE to NoiseAR [43], which is a costlier (compared to Naïve PAINE and [90]), RLHF and fine-tuning approach that performs initial noise optimization by modifying the DM noise after every timestep in an autoregressive manner.

As we can see from Table, Naïve PAINE achieves competitive performance on several DMs such as Hunyuan and PixArt- Σ especially, across a variety of prompt sets and preference scores like HPSv2 or v3. Specifically, Naïve PAINE achieves the best performance in over 22 of 64 test scenarios and the second best performance in over 30 scenarios. Overall, these results further corroborate the efficacy and viability of Naïve PAINE as an effective method for achieving initial noise optimization.

Full GenEval comparison. Next, Table 8 expands upon Table 2 to provide a full slew of categorical results on the GenEval [22] benchmark. We observe that in general, Naïve PAINE achieves competent performance in several evaluation categories, specifically single or two object generation, as well as colors and position. Overall, like before, Naïve PAINE achieves the second-best performance, only behind NoiseAR on three of four DMs. This finding is impressive considering NoiseAR is a costlier fine-tuning-based method and we did not optimize Naïve PAINE for GenEval, but PickScore [38] primarily.

Table 7: T2I Quantitative Comparison on several human preference benchmarks and prompt datasets. Same setup as Table 1. Best and second best results in **bold** and *italics*, respectively.

Model	Dataset	Method	HPSv2 (\uparrow)	HPSv3 (\uparrow)	ImageReward (\uparrow)	PickScore (\uparrow)
Hunyuan	Pick-a-Pic	Standard	29.48	8.06	85.47	21.81
		NoiseAR	<i>30.27</i>	8.56	103.7	21.93
		Naïve PAINE	30.77	<i>8.24</i>	<i>89.52</i>	<i>21.86</i>
	HPDv2	Standard	31.04	10.01	109.27	22.88
		NoiseAR	<i>31.42</i>	10.17	121.17	23.01
		Naïve PAINE	32.79	<i>10.02</i>	<i>114.78</i>	<i>23.00</i>
	HPSv2	Standard	30.06	11.42	106.41	<i>22.58</i>
		NoiseAR	<i>30.32</i>	11.60	116.05	22.63
		Naïve PAINE	31.70	<i>11.43</i>	<i>108.42</i>	<i>22.58</i>
	DrawBench	Standard	28.49	<i>9.18</i>	84.45	22.31
		NoiseAR	<i>29.14</i>	9.53	<i>89.53</i>	22.48
		Naïve PAINE	30.16	9.10	89.88	<i>22.33</i>
PixArt- Σ	Pick-a-Pic	Standard	29.83	<i>8.60</i>	81.24	21.90
		NoiseAR	<i>29.91</i>	8.18	<i>84.58</i>	21.71
		Naïve PAINE	30.82	8.73	86.02	<i>21.82</i>
	HPDv2	Standard	30.91	<i>10.53</i>	106.45	<i>22.98</i>
		NoiseAR	<i>31.88</i>	9.75	102.93	22.78
		Naïve PAINE	32.71	10.58	<i>106.11</i>	23.01
	HPSv2	Standard	<i>31.70</i>	<i>11.93</i>	<i>103.21</i>	<i>22.68</i>
		NoiseAR	30.57	11.07	96.47	22.38
		Naïve PAINE	31.79	11.96	103.23	22.70
	DrawBench	Standard	28.54	9.60	<i>73.41</i>	<i>22.33</i>
		NoiseAR	<i>28.92</i>	8.66	60.12	22.13
		Naïve PAINE	30.03	<i>9.57</i>	75.60	22.34
DreamShaper	Pick-a-Pic	Standard	32.51	<i>10.33</i>	98.06	22.60
		NoiseAR	33.64	10.44	111.12	22.71
		Naïve PAINE	<i>33.27</i>	10.29	<i>106.60</i>	<i>22.64</i>
	HPDv2	Standard	33.95	12.38	129.51	23.88
		NoiseAR	<i>34.66</i>	<i>12.34</i>	<i>131.85</i>	<i>23.70</i>
		Naïve PAINE	34.85	12.01	119.49	23.59
	HPSv2	Standard	34.39	13.90	121.91	23.42
		NoiseAR	34.65	13.97	126.23	23.48
		Naïve PAINE	<i>34.44</i>	<i>13.94</i>	<i>123.24</i>	<i>23.44</i>
	DrawBench	Standard	30.17	11.57	96.37	22.92
		NoiseAR	<i>31.05</i>	11.71	106.56	23.05
		Naïve PAINE	31.58	<i>11.70</i>	<i>97.28</i>	<i>22.93</i>
SDXL	Pick-a-Pic	Standard	28.40	7.10	57.94	21.65
		NoiseAR	29.07	<i>7.39</i>	<i>75.29</i>	21.85
		Naïve PAINE	<i>28.85</i>	7.90	80.86	<i>21.82</i>
	HPDv2	Standard	29.66	8.73	82.66	22.83
		NoiseAR	<i>30.77</i>	9.45	108.04	23.05
		Naïve PAINE	31.70	<i>8.95</i>	<i>100.78</i>	<i>22.93</i>
	HPSv2	Standard	<i>28.69</i>	<i>10.24</i>	85.06	22.52
		NoiseAR	29.10	10.56	96.07	<i>22.65</i>
		Naïve PAINE	28.67	10.21	<i>92.37</i>	23.01
	DrawBench	Standard	26.83	7.88	60.08	22.28
		NoiseAR	<i>27.72</i>	8.40	71.31	22.60
		Naïve PAINE	28.66	<i>8.16</i>	<i>66.00</i>	<i>22.31</i>

Table 8: Full quantitative Performance on GenEval [22] across all categories. Best and second best results in **bold** and *italics*, respectively.

Model	Method	Single Obj. (↑)	Two Obj. (↑)	Counting (↑)	Colors (↑)	Position (↑)	Color Attrib. (↑)	Overall (↑)
Hunyuan	Standard	<i>97.81</i>	82.83	61.25	88.30	<i>17.75</i>	46.75	<i>65.78</i>
	Golden Noise	97.19	81.57	<i>62.19</i>	89.36	18.00	47.75	66.00
	NoiseAR	98.44	<i>83.03</i>	66.88	89.36	12.00	44.75	65.75
	Naïve PAINE	97.19	83.59	59.38	<i>88.56</i>	15.00	<i>47.50</i>	65.20
PixArt- Σ	Standard	<i>99.06</i>	60.86	47.19	85.37	15.25	25.00	55.45
	Golden Noise	98.75	61.87	47.19	82.71	12.25	28.00	55.12
	NoiseAR	98.75	<i>63.89</i>	58.44	81.12	12.75	21.75	56.16
	Naïve PAINE	99.38	65.15	<i>49.38</i>	<i>83.51</i>	<i>14.00</i>	<i>25.25</i>	<i>56.11</i>
DreamShaper	Standard	100	<i>82.83</i>	<i>44.69</i>	84.84	<i>13.25</i>	30.00	59.26
	Golden Noise	100	85.35	41.56	85.90	11.50	<i>30.75</i>	59.18
	NoiseAR	100	85.35	40.94	<i>85.64</i>	15.50	32.00	59.90
	Naïve PAINE	100	80.56	45.31	85.90	<i>13.25</i>	29.25	<i>59.38</i>
SDXL	Standard	<i>98.12</i>	71.21	37.81	83.78	9.25	<i>21.50</i>	53.61
	Golden Noise	98.75	67.68	37.50	<i>82.98</i>	<i>13.00</i>	21.00	53.49
	NoiseAR	96.25	77.78	43.44	82.91	11.25	27.56	55.08
	Naïve PAINE	<i>98.12</i>	<i>72.22</i>	<i>40.00</i>	82.21	18.15	19.50	<i>54.05</i>

Table 9: SANA-Sprint T2I evaluation on five prompt benchmarks. Naïve PAINE is trained on PickScore. Best results in **bold**, second best in *italics*.

Dataset	Method	HPSv2 (↑)	PickScore (↑)	ImageReward (↑)	HPSv3 (↑)
Pick-a-Pic	Standard	30.10	22.03	94.64	8.69
	HyperNoise	32.31	21.92	125.07	8.84
	Naïve PAINE	<i>30.83</i>	22.00	<i>98.61</i>	8.85
HPDv2	Standard	32.03	23.04	93.20	11.14
	HyperNoise	34.25	<i>23.05</i>	133.20	11.71
	Naïve PAINE	<i>32.23</i>	22.96	<i>106.36</i>	<i>11.27</i>
HPSv2	Standard	30.13	22.73	105.47	12.59
	HyperNoise	33.38	<i>22.74</i>	133.79	13.30
	Naïve PAINE	<i>31.53</i>	22.77	<i>107.25</i>	<i>12.73</i>
DrawBench	Standard	28.58	<i>22.48</i>	90.86	10.52
	HyperNoise	31.27	22.43	113.41	<i>11.04</i>
	Naïve PAINE	<i>30.07</i>	22.47	<i>86.74</i>	10.92

C SANA-Sprint

We further compare Naïve PAINE to an HyperNoise [19]. This approach is more akin to NoiseAR [43] in that it is a RLHF and fine-tuning-based initial noise optimization approach, requiring up to 6 H100 GPUs to execute, rather than Naïve PAINE and Golden Noise [90] which are fine-tuning-free and only require a single consumer-grade GPU. However, different from NoiseAR, HyperNoise is tailored towards few-step [70] DMs, some of which utilize radically different latent spaces [18, 85] than what we consider in the main paper, so an additional comparison helps to further demonstrate the robustness of our method.

Specifically, we extend Naïve PAINE to SANA-Sprint [11], a single-step DM whose latent space consists of 32 channels with higher downsampling, as opposed to prior results which work within the 4 channel latent space of SDXL. Naïve PAINE trains a standalone predictor on PickScore as the target metric using the same procedure as the other DMs (Section A.1).

Table 9 provides the qualitative results comparing Naïve PAINE to HyperNoise on a variety of T2I prompt sets and preference metrics. Naïve PAINE outperforms HyperNoise on several prompt sets and preference metrics, e.g., Pick-a-Pic and DrawBench, while also providing competitive performance on HPDv2 and HPSv2. Thus, these results demonstrate not only the generalizability of Naïve PAINE to generate high-quality artwork on DMs that utilize different latent spaces, but to do so competitively against methods that require much heftier initial upfront compute investment to fine-tune specific DMs.

Additionally, Figure 8 provides some qualitative examples on SANA-Sprint comparing Naïve PAINE to HyperNoise and the standard, optimization-free baseline. These results further illustrate the deployment efficacy and competitiveness of our method.

Standard

HyperNoise

Naïve PAINE



“Teenage boy wearing a skull mask and smoking.”



“A Wojack looking over a sea of memes from a cliff on 4chan.”



“A racoon riding an oversized fox through a forest in a furry art anime still.”

Fig. 8: Qualitative results comparing Naïve PAINE to HyperNoise on SANA-Spring. All prompts from HPDv2 [84].

D Additional Ablation Studies

We extend our initial ablation results from Section 4.4 with Table 10. Specifically, this table ablates four independent design choices of Naïve PAINE and evaluate the resulting predictors on the PickScore test set using the SDXL DM unless otherwise stated. In all cases the default configuration matches the model reported in the main paper.

Table 10: Ablation studies on SDXL with Pick-a-Pic evaluation benchmark. We select PickScore as the default target, $N=100$ candidate noises, and MAE+SRCC as the default loss because this combination yields consistently competitive scores across all four metrics without sacrificing performance on any individual one. Best results **bolded**.

Ablation	Variant	HPSv2 (↑)	HPSv3 (↑)	ImageReward (↑)	PickScore (↑)
Predictor Target	HPSv2	28.69	7.09	61.79	21.7
	PickScore	28.85	7.90	72.00	21.81
	ImageReward	29.85	7.28	58.26	21.77
Loss Function	MAE + SRCC	28.85	7.90	72.00	21.81
	MAE + LambdaRank	28.97	7.03	80.86	21.80
N Sensitivity	$N = 50$	30.01	7.43	76.04	21.7
	$N = 100$	28.85	7.90	72.00	21.81
	$N = 500$	29.83	7.23	70.82	21.75
Text Encoder	AttnPool	28.85	7.90	72.00	21.81
	PerTokenScalar	30.11	7.36	70.48	21.79

D.1 Predictor Target Metric

The first segment of Tab. 10 quantifies Figure 6 with actual numerical values. Specifically, we train three predictors on SDXL using HPSv2 [84], PickScore [38], and ImageReward [86] as the regression target while keeping all other hyperparameters fixed (`mae+srcc` loss, $N=100$, AttnPool text encoder). As shown in Figure 6 of the main paper, training with PickScore as the target yields the best overall downstream PickScore performance on generated images. This pattern is consistent: the predictor generalizes best to the metric it was trained to rank.

D.2 Loss Function

The second section of Tab. 10 considers the loss function utilized to train Naïve PAINE. Specifically, we compare two loss configurations: (i) MAE + differentiable SRCC (`mae+srcc`), and (ii) MAE + LambdaRank (`mae+lambdaRank`). In the LambdaRank variant, the MAE loss provides standard gradient flow, while the LambdaRank gradient directly optimizes NDCG@3 via list-wise weighting of pairwise prediction errors. Both losses operate per-prompt group using the grouped batch sampler. Results show that `mae+srcc` is the stronger default across DMs and metrics.

D.3 N Sensitivity

The third segment of Tab. 10 considers the choice of N when generating a single image, $|B| = 1$. Specifically, we evaluate sensitivity to the number of candidate noises N by testing $N \in \{50, 100, 500\}$ at inference time. All predictors are trained identically (PickScore target, `mae+srcc` loss, AttnPool); only the number of noises scored per prompt at test time varies. The results indicate that performance saturates around $N=100$ and increasing to $N=500$ yields diminishing returns, motivating our default choice of $N=100$. Further, per Tab. 4,

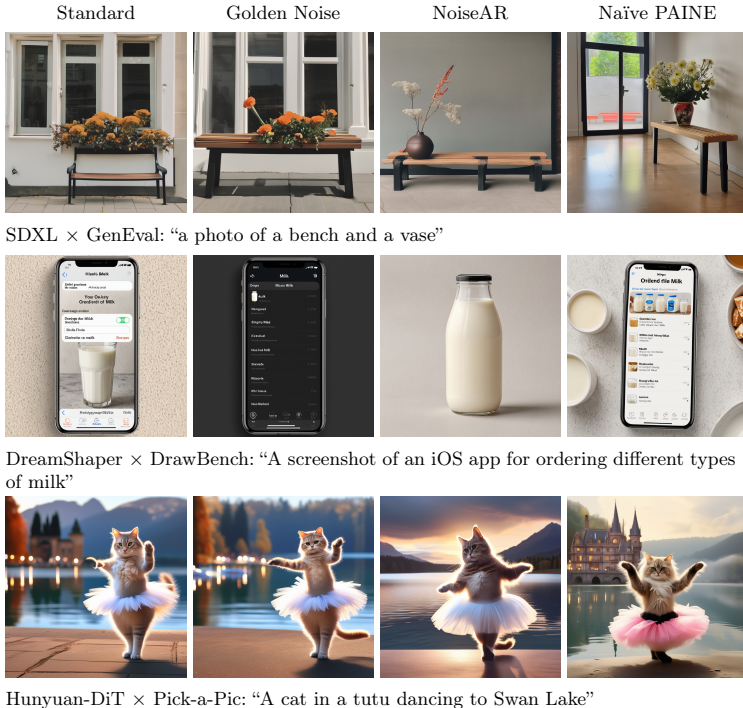


Fig. 9: Additional qualitative examples comparing Naïve PAINE to Golden Noise, NoiseAR and the standard baseline. DM and prompt details provided below each row.

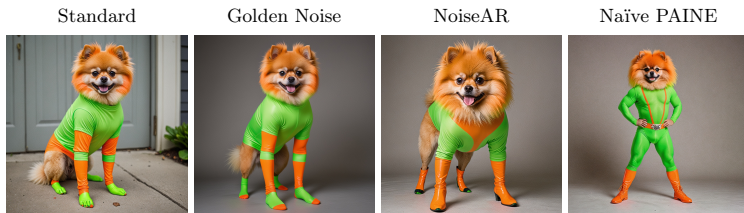
even at $N = 100$, we typically achieve lower hardware latency than other noise optimization methods.

D.4 Text Encoder Architecture

Finally, the last segment of Tab. 10 considers the architecture of the PAINE prompt embedding neural network Φ_{prompt} . Specifically, we compare two text encoder designs: (i) the proposed **AttnPool** encoder (learnable summary token + 2 self-attention blocks, 16 heads) and (ii) **PerTokenScalar**, a simpler per-token MLP that projects each token embedding to a scalar and aggregates them. **AttnPool** consistently outperforms **PerTokenScalar**, which we attribute to the attention mechanism’s ability to model inter-token dependencies and focus on semantically salient tokens rather than treating each token independently.

E Additional PAINE Examples

We provide additional image examples in Figs. 9 and 10.



DreamShaper \times DrawBench: “A realistic photo of a Pomeranian dressed up like a 1980s professional wrestler with neon green and neon orange face paint and bright green wrestling tights with bright orange boots.”



Hunyuan-DiT \times Pick-a-Pic: “a majestic vicious dragon habitat landscape, boss fight scene, refractions, realistic, cinematic lighting, antview, natural, horrific atmosphere, sharp focus”



Hunyuan-DiT \times Pick-a-Pic: “Movie Still of the Joker wielding a red Lightsaber, Darth Vader a sinister evil clown prince of crime, HD photograph”



SDXL \times Pick-a-Pic: “Detailed Ink splash portrait of a Lion: Alex maleev: Ashley Wood: Carne Griffiths: oil painting: high contrast: COLORFUL: 3D: ultra-fine details: dramatic lighting: fantastical: sharp focus: Daniel dociu: splash art: professional photography: Artur N. Kisteb: ZBrushCentral: finalRender: Unreal Engine 5: Trending on Artstation: Jeff Koons: Deep colors: deep depth of field”



PixArt- Σ \times HPDv2: “Popcorn in mouth”

Fig. 10: Additional qualitative image examples.